2011

Effect of thermal strain on J(c) and T-c in high density nano-SiC doped MgB2

Wenxian Li
University of Wollongong, wenxian@uow.edu.au

Rong Zeng
University of Wollongong, rzeng@uow.edu.au

Lin Lu
University of Wollongong, ll972@uowmail.edu.au

S. X. Dou
University of Wollongong, shi@uow.edu.au

Effect of thermal strain on Jc and Tc in high density nano-SiC doped MgB2

W. X. Li, R. Zeng, L. Lu, and S. X. Dou

Citation: J. Appl. Phys. **109**, 07E108 (2011); doi: 10.1063/1.3549590
View online: http://dx.doi.org/10.1063/1.3549590
View Table of Contents: http://jap.aip.org/resource/1/JAPIAU/v109/i7
Published by the American Institute of Physics.

Effect of thermal strain on J_c and T_c in high density nano-SiC doped MgB_2

W. X. Li, R. Zeng, L. Lu, and S. X. Dou[a)]
Institute for Superconducting and Electronic Materials, University of Wollongong, Northfields Avenue, Wollongong NSW 2522, Australia

(Presented 16 November 2010; received 21 September 2010; accepted 12 November 2010; published online 21 March 2011)

The influences of lattice strain on the superconducting critical current density J_c and critical transition temperature T_c in pure MgB_2 and a SiC-MgB_2 composite made by the diffusion process are explored, based on the thermal expansion coefficients and the low temperature effects on Raman scattering. The strong thermal strain provides a strong flux pinning force for the supercurrents at the interfaces between SiC and MgB_2. The high T_c of SiC-MgB_2 is also discussed according to the expanded lattice and Raman characteristics. © *2011 American Institute of Physics*. [doi:10.1063/1.3549590]

MgB_2 shows great potential for application in superconducting coils due to its relatively high critical temperature, T_c, which allows the use of simple and inexpensive cryocoolers. The improvement of critical current density in high magnetic fields depends on efficient pinning centers.[1] High crystal connectivity and high density are beneficial to T_c and the critical current density J_c, for MgB_2 bulks fabricated using the *in situ* diffusion process.[2] Doping nano-SiC particles into MgB_2 has been proven to be particularly effective in significantly enhancing J_c, the irreversibility field, H_{irr}, and the upper critical field, H_{c2}.[3–5] In contrast to chemical doping effects, tensile stress is believed to act as a source of strong flux pinning centers when there is no reaction between SiC and MgB_2. Both the J_c and T_c are improved by thermal strain on the interface between SiC and MgB_2 during the diffusion process[2] and hybrid physical-chemical vapor deposition.[6] In this paper, microstructural analysis and Raman scattering measurements are employed to investigate the origin of the huge flux pinning force. The effects of the stress field on the flux pinning and electron-phonon coupling are discussed to explain the behavior of a high density SiC-MgB_2 composite made by the diffusion process.

Crystalline B (99.999%) powders, with and without 10 wt. % SiC particles, were mixed and pressed into pellets. The pellets were then put into iron tubes filled with Mg powder (99.8%). The atomic ratio of Mg to B was 1.15:2.0. Considering the time dependence of the diffusion process, sintering was conducted at 1123 K for 10 h under a flow of high purity argon gas to achieve fully reacted MgB_2 bulks. The SiC particles remained un-reacted and formed a composite with the MgB_2 in the SiC-doped sample, judging from the absence of Mg_2Si in the x-ray diffraction (XRD) patterns. The Rietveld refinement results showed that the un-reacted SiC represented about 9.3 wt. %, which is about the same as in the precursor. This result is different from what is seen in SiC doped MgB_2 prepared by the usual *in situ* technique,[3,7] in which only a very small amount of SiC remains, while Mg_2Si is always present due to the reaction of Mg with SiC. For the present samples produced by diffusion, the *a*- and *c*-axis lattice parameters were 3.0850 Å and 3.5230 Å for the pure MgB_2, and 3.0840 Å and 3.5282 Å for the SiC doped MgB_2, respectively. The *a*-axis parameters are virtually equivalent for the two samples, whereas the *c*-axis parameter is slightly enlarged in the SiC-MgB_2 composite. In contrast, the *a*-axis parameter for the usual *in situ* processed SiC doped MgB_2 is reduced, while the *c*-axis parameter should remain unchanged.[3,8]

To explain the abnormal *c*-axis enlargement of the SiC-MgB_2 composite, the thermal expansion coefficients α of MgB_2 and SiC need to be considered.[2] It is reasonable to assume that both the MgB_2 and the SiC are in a stress-free state at the sintering temperature of 1123 K due to the relatively high sintering temperature over a long period of time. However, the lattice parameters are determined by the thermal strain during the cooling process. The α_{SiC} decreases slightly from 5×10^{-6}/K at 1123 K to 2.5×10^{-6}/K at 0 K, whereas the α_{MgB_2} drops quickly from 1.7×10^{-5}/K at 1123 K to zero at 0 K. The normalized lattice strain is estimated to be −0.55% in SiC-MgB_2 along the *c*-axis at room temperature. The negative value corresponds to tensile strain in the MgB_2. The large *c*-axis strain in the doped MgB_2 resulted in an enlargement of the *c*-axis parameter by 0.15% in comparison with pure MgB_2. Figure 1 shows a transmission electron microscope image of an interface between SiC and MgB_2. Based on the fast Fourier transform analysis, the interface is marked by a dashed line on the image. The right side is a SiC grain parallel to the [101] plane and the left side is an MgB_2 grain parallel to the [001] plane. This kind of interface will impose tensile stress along the *c*-axis in MgB_2, which is responsible for the enlarged *c*-axis parameter of MgB_2.

Based on the collective pinning model,[9] J_c is independent of the applied field in the single-vortex pinning regime (low magnetic field region: $H < H_{sb}$), where H_{sb} is the crossover field from single-vortex to small-bundle pinning. The J_c decreases exponentially in the small-bundle regime (high magnetic field: $H_{sb} < H < H_{irr}$). According to the dual model,[3] the significant effect of SiC doping on J_c comes

a)Author to whom correspondence should be addressed. Electronic mail: shi@uow.edu.au.

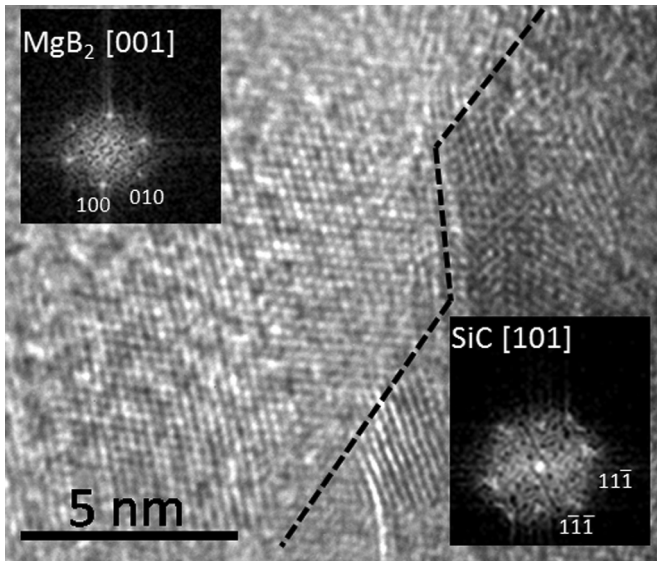

FIG. 1. High resolution TEM image of the interface in SiC-MgB_2 and (inset) fast Fourier transform patterns of SiC and MgB_2 from each side of the interface. The dashed line indicates the interface of SiC and MgB_2.

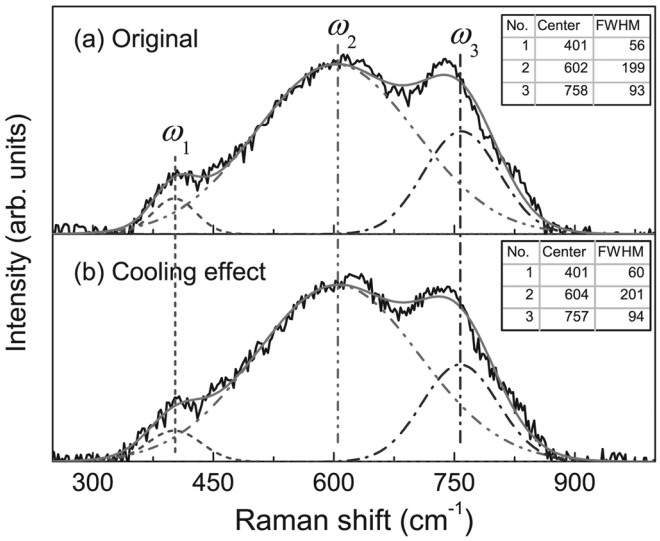

FIG. 3. (a) Fitting and experimental results for the normalized ambient Raman spectrum of MgB_2 sintered at 850 °C for 10 h, and (b) the cooling effect on the Raman spectrum.

from the high level of C substitution on the B plane, which is responsible for the reduction of the self-field J_c.[4,5] However, the SiC-MgB_2 composite sample shows not only an improved in-field J_c, but also no degradation in self-field J_c, as indicated in Fig. 2. The approximate H_{sb} values are also indicated on the J_c curves for 20 K and 30 K, although H_{sb} has not been detected at 5 K due to the relatively high supercurrents. The *in situ* processed SiC doped MgB_2 normally shows a decrease in T_c of 1.5 to 2 K,[3–5] but this present SiC-MgB_2 composite sample shows a small drop of 0.6 K, as shown in the inset of Fig. 2. This phenomenon is attributed to the absence of any reaction between Mg and SiC, as well as the stretched MgB_2 lattice, as indicated by the XRD pattern.[6]

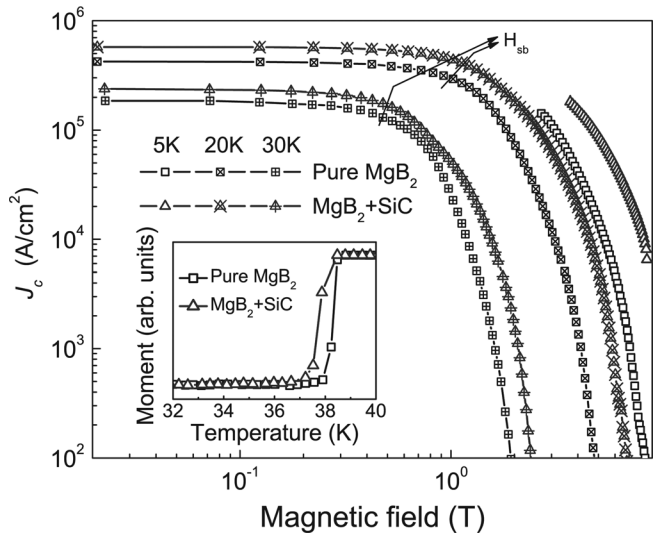

FIG. 2. The magnetic J_c versus field at 5 K, 20 K, and 30 K for pure and nano-SiC doped samples. The inset shows the superconducting transition of the two samples.

To investigate whether the lattice strain is significant in SiC-MgB_2 during low temperature measurements to obtain $M(H)$ and $M(T)$ curves, Raman spectra were collected before and after the measurements with a confocal laser Raman spectrometer (Renishaw inVia plus) under a 100 × microscope. The 514.5 nm line of an Ar^+ laser was used for excitation. The Raman spectra for pure MgB_2 are shown in Figs. 3(a) and 3(b) to compare the cooling effects on the matrix. Both of the spectra have been fitted with three peaks: ω_1, ω_2, and ω_3.[10–12] Based on the previous results, ω_2 is the reflection of the E_{2g} mode at the Γ point of the Brillouin zone in the simple hexagonal MgB_2 structure (space group: *P6/mmm*), while ω_1 and ω_3 come from the lattice distortion. The effects of ω_1 are not discussed in the following analysis because of its small influence on the spectra. As indicated by the fitting parameters that are shown in Fig. 3, both the peak centers and the full width at half maximum (FWHM) values show negligible differences before and after the low temperature measurements due to synchronic volume fluctuation. The weak temperature dependence of the Raman spectra for pure MgB_2 is in agreement with the results of Shi *et al.*[13] The ω_2 peak of the Raman spectrum of SiC-MgB_2 before the low temperature measurement has shifted to the low frequency of 585 cm^{-1}, as shown in Fig. 4(a). The FWHM of the ω_2 peak increases from ~200 cm^{-1} to 210 cm^{-1}. Furthermore, the FWHM of the ω_3 peak increases from ~93 cm^{-1} to 125 cm^{-1}. The variations of both the Raman shift and the FWHM indicate the strong lattice strain in the SiC-MgB_2 composite. Figure 4(b) shows the cooling effect on the Raman spectrum of SiC-MgB_2. The FWHM of the ω_2 peak further increases to 228 cm^{-1}, and the frequency of ω_3 peak shifts to 770 cm^{-1}. These results suggest that the stress field is very strong during the low temperature measurements in the SiC-MgB_2 composite. Considering the stable defect structures in the sample at room temperature and the measurement temperatures, the high J_c performance is attributed to the thermal strain. Although the

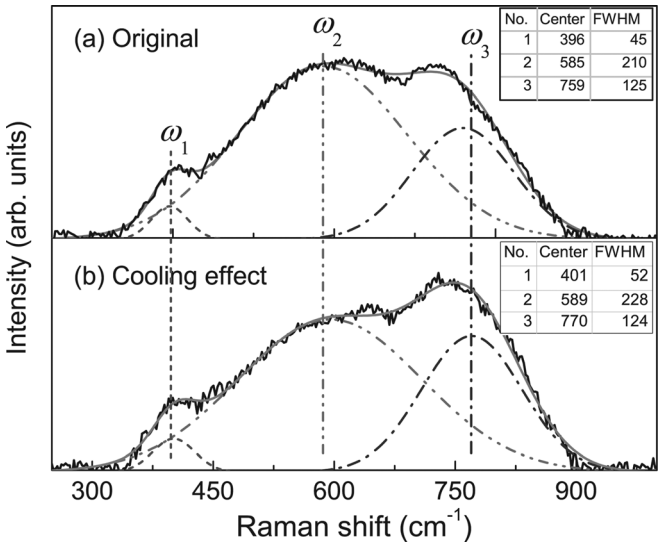

FIG. 4. (a) Fitting and experimental results for the normalized ambient Raman spectrum of SiC-MgB_2 sintered at 850 °C for 10 h, and (b) the cooling effect on the Raman spectrum.

interface or grain boundaries themselves are effective flux pinning centers, the thermal strain provides a more efficient flux pinning force, based on the comparison of the J_c values in pure MgB_2 and the SiC-MgB_2 composite.

It should be noted that the broadened ω_2 peak in SiC-MgB_2 is a signal of strong electron-E_{2g} coupling, which is responsible for the high T_c in MgB_2. The electron-E_{2g} coupling constant is estimated from the Allen equation:[14] $\Gamma_2 = 2\pi\lambda_{E_{2g}} N(0)\omega^2_{E_{2g}}$, where Γ_2 is the ω_2 linewidth, $\lambda_{E_{2g}}$ is the strength of the electron-E_{2g} coupling, and $N(0)$ is the density of states on the Fermi-surface, which is the only electronic property explicitly occurring in this equation. The measured phonon frequency and phonon linewidth, in the absence of anharmonic contributions, are simply and directly related to the electron-phonon coupling (EPC) constant, $\lambda_{E_{2g}}$. The total density of states at the Fermi energy, E_F, in pure MgB_2 is taken as $N(0) = 0.354$ states/eV/cell/spin, with the contribution from the σ band being 0.15 and that from the π band being 0.204.[15] $N(0)$ is assumed to be constant for the small changes of electrons and holes in MgB_2 and SiC-MgB_2. Taking the fitting values of the ω_2 peaks with cooling effects, the $\lambda_{E_{2g}}$ values for the pure MgB_2 and SiC-MgB_2 are 2.327 and 2.706, respectively. The $\lambda_{E_{2g}}$ of SiC-MgB_2 is just slightly higher than that of the pure MgB_2. However, the T_c of SiC-MgB_2 is decreased slightly compared to that of the pure MgB_2. The total EPC constants are degraded by the scattering effects of SiC impurities in the MgB_2 matrix, which can be estimated with the McMillan formula,[16] as modified by Allen and Dynes:[17] $T_c = \langle\omega_{\log}\rangle/1.2\exp[-1.04(1+\lambda)/\lambda - \mu^*(1+0.62\lambda)]$, where $\langle\omega_{\log}\rangle = (390\times\omega^2_{E_{2g}}\times 690)$ is the averaged phonon frequency,[18] with 390 and 690 cm^{-1} being the phonon frequencies of the other modes in the MgB_2 system,[19] μ^* is the Coulomb pseudopotential, taken as equal to 0.13,[20] and λ is the total EPC constant. Using these values, λ is calculated as 0.888 in pure MgB_2 and 0.886 in SiC-MgB_2, respectively. Although the values are very similar, the λ of MgB_2 is a little higher because of its low impurity scattering effects. The residual resistivity of SiC-MgB_2 is 16 $\mu\Omega\cdot$cm, but it is just 12 $\mu\Omega\cdot$cm for pure MgB_2, due to the weak impurity scattering effects.

In summary, the thermal strain originating from the interface of SiC and MgB_2 is one of the most effective sources of flux pinning centers to improve the supercurrent critical density. The weak temperature dependence of the thermal expansion coefficient of SiC stretches the MgB_2 lattice as the temperature decreases. The thermal strain supplies much more effective flux pinning force than the interfaces and grain boundaries themselves. The low temperature effects on Raman spectra show very strong lattice stretch at the application temperature of MgB_2, which benefits both the J_c and the T_c behaviors.

The authors thank Dr. T. Silver for her useful discussions and Dr. R. K. Zheng for his microstructure observation. This work is supported by the Australian Research Council (project ID: DP0770205) and Hyper Tech Research Inc.

[1]A. Gumbel, J. Eckert, G. Fuchs, K. Nenkov, K. H. Muller, and L. Schultz, Appl. Phys. Lett. **80**, 2725 (2002).
[2]R. Zeng, S. X. Dou, L. Lu, W. X. Li, J. H. Kim, P. Munroe, R. K. Zheng, and S. P. Ringer, Appl. Phys. Lett. **94**, 042510 (2009).
[3]S. X. Dou, O. Shcherbakova, W. K. Yeoh, J. H. Kim, S. Soltanian, X. L. Wang, C. Senatore, R. Flukiger, M. Dhalle, O. Husnjak, and E. Babic, Phys. Rev. Lett. **98**, 097002 (2007).
[4]W. X. Li, R. Zeng, L. Lu, Y. Li, and S. X. Dou, J. Appl. Phys. **106**, 093906 (2009).
[5]W. X. Li, R. Zeng, L. Lu, Y. Zhang, S. X. Dou, Y. Li, R. H. Chen, and M. Y. Zhu, Physica C **469**, 1519 (2009).
[6]A. V. Pogrebnyakov, J. M. Redwing, S. Raghavan, V. Vaithyanathan, D. G. Schlom, S. Y. Xu, Q. Li, D. A. Tenne, A. Soukiassian, X. X. Xi, M. D. Johannes, D. Kasinathan, W. E. Pickett, J. S. Wu, and J. C. H. Spence, Phys. Rev. Lett. **93**, 147006 (2004).
[7]A. Matsumoto, H. Kumakura, H. Kitaguchi, B. J. Senkowicz, M. C. Jewell, E. E. Hellstrom, Y. Zhu, P. M. Voyles, and D. C. Larbalestier, Appl. Phys. Lett. **89**, 132508 (2006).
[8]M. D. Sumption, M. Bhatia, M. Rindfleisch, M. Tomsic, S. Soltanian, S. X. Dou, and E. W. Collings, Appl. Phys. Lett. **86**, 092507 (2005).
[9]G. Blatter, M. V. Feigelman, V. B. Geshkenbein, A. I. Larkin, and V. M. Vinokur, Rev. Mod. Phys. **66**, 1125 (1994).
[10]W. X. Li, Y. Li, R. H. Chen, R. Zeng, M. Y. Zhu, H. M. Jin, and S. X. Dou, J. Phys.: Condens. Matter **20**, 255235 (2008).
[11]W. X. Li, Y. Li, R. H. Chen, R. Zeng, S. X. Dou, M. Y. Zhu, and H. M. Jin, Phys. Rev. B **77**, 094517 (2008).
[12]W. X. Li, R. Zeng, C. K. Poh, Y. Li, and S. X. Dou, J. Phys.: Condens. Matter **22**, 135701 (2010).
[13]L. Shi, H. R. Zhang, L. Chen, and Y. Feng, J. Phys.: Condens. Matter **16**, 6541 (2004).
[14]P. B. Allen, Phys. Rev. B **6**, 2577 (1972).
[15]J. Kortus, O. V. Dolgov, R. K. Kremer, and A. A. Golubov, Phys. Rev. Lett. **94**, 027002 (2005).
[16]W. L. McMillan, Phys. Rev. **167**, 331 (1968).
[17]P. B. Allen and R. C. Dynes, Phys. Rev. B **12**, 905 (1975).
[18]J. Kortus, I. I. Mazin, K. D. Belashchenko, V. P. Antropov, and L. L. Boyer, Phys. Rev. Lett. **86**, 4656 (2001).
[19]R. Osborn, E. A. Goremychkin, A. I. Kolesnikov, and D. G. Hinks, Phys. Rev. Lett. **87**, 017005 (2001).
[20]A. Brinkman, A. A. Golubov, H. Rogalla, O. V. Dolgov, J. Kortus, Y. Kong, O. Jepsen, and O. K. Andersen, Phys. Rev. B **65**, 180517 (2002).